Advances in Energy Research, *Vol. 6, No. 1 (2019) 75-90*
DOI: http://ddoi.org/10.12989/eri.2019.6.1.075

Geomechanical assessment of reservoir and caprock in CO_2 storage: A coupled THM simulation

Roohollah Taghizadeh[1], Kamran Goshtasbi[*2], Abbas Khaksar Manshad[3] and Kaveh Ahangari[1]

[1]Department of Mining Engineering, Science and Research Branch, Islamic Azad University, Tehran, Iran
[2]Department of Mining Engineering, Faculty of Engineering, Tarbiat Modares University, Tehran, Iran
[3]Department of Petroleum Engineering, Faculty of Petroleum Engineering, Petroleum University of Technology, Abadan, Iran

(Received April 24, 2018, Revised May 25, 2019, Accepted May 26, 2019)

Abstract. Anthropogenic greenhouse gas emissions are rising rapidly despite efforts to curb release of such gases. One long term potential solution to offset these destructive emissions is the capture and storage of carbon dioxide. Partially depleted hydrocarbon reservoirs are attractive targets for permanent carbon dioxide disposal due to proven storage capacity and seal integrity, existing infrastructure. Optimum well completion design in depleted reservoirs requires understanding of prominent geomechanics issues with regard to rock-fluid interaction effects. Geomechanics plays a crucial role in the selection, design and operation of a storage facility and can improve the engineering performance, maintain safety and minimize environmental impact. In this paper, an integrated geomechanics workflow to evaluate reservoir caprock integrity is presented. This method integrates a reservoir simulation that typically computes variation in the reservoir pressure and temperature with geomechanical simulation which calculates variation in stresses. Coupling between these simulation modules is performed iteratively which in each simulation cycle, time dependent reservoir pressure and temperature obtained from three dimensional compositional reservoir models in ECLIPSE were transferred into finite element reservoir geomechanical models in ABAQUS and new porosity and permeability are obtained using volumetric strains for the next analysis step. Finally, efficiency of this approach is demonstrated through a case study of oil production and subsequent carbon storage in an oil reservoir. The methodology and overall workflow presented in this paper are expected to assist engineers with geomechanical assessments for reservoir optimum production and gas injection design for both natural gas and carbon dioxide storage in depleted reservoirs.

Keywords: permanent disposal; seal integrity; geomechanics; caprock integrity; stress; coupling

1. Introduction

Minimizing climate change impacts from increasing atmospheric carbon dioxide (CO_2)

---

*Corresponding author, Associate Professor, E-mail: goshtasb@modares.ac.ir
[a]Ph.D. Student, E-mail: r.taghizadeh1978@yahoo.com
[b]Assistatnt Professor, E-mail: khaksar@put.ac.ir
[c]Associate Professor, E-mail: kaveh.ahangari@gmail.com

http://www.techno-press.org/?journal=eri&subpage=7 ISSN: 2287-6316 (Print), 2287-6324 (Online)

concentrations calls for dramatic reductions in anthropogenic CO_2 emissions if stabilization is to be accomplished (Hoffert *et al.* 2002, Pacala and Socolow 200, IPCC 2007). In past years, a number of ideas have been proposed to cope with the problem, among which geological storage method is one of the most viable solutions (House *et al.* 2006). The technology involves the capture of CO_2 emissions and the storage in suitable underground porous geological formations for long periods of time.

Geomechanical effects associated with CO_2 injection are caused by pore pressure build-up and cooling of the injection reservoirs when the temperature of injected CO_2 is lower than the ambient rock temperature. Pressure increase and cooling induce poro-elastic and thermal stresses that alter the pre-injection state of stress within and beyond the pressure- and cooling affected areas (Goodarzi *et al.* 2010, Elyasi *at al.* 2016a, b). Pressure and stress changes result in rock deformation which may impact seal integrity. These geomechanical effects must be evaluated in order to ensure containment and to assess leakage-incurred risks. In some cases, injection-induced deformation can be benign, thus not posing a threat to the integrity of overlying sealing formations and the containment (Elyasi *et al.* 2016c, Chadwick *et al.* 2012). In other cases, CO_2 injection can lead to significant geomechanical responses, causing reactivation of pre-existing fractures and faults in the reservoir and, even more importantly, in overlying sealing formations. Forecasting such effects requires a 3-dimensional (3D) geomechanical model of the site describing in situ rock stresses, fluid pressure, poro-elastic and strength properties of the formations. Initial conditions at static equilibrium are computed. This mechanical model is linked to a reservoir model to further simulate the stress path, deformations and potential failure associated with a given CO_2 injection scenario.

In this paper, we want to evaluate how geomechanics influence the storage capacity and seal integrity of a reservoir through the lifetime of the field. In order to do so, we have linked two codes, ECLIPSE and ABAQUS for assessment of coupled THM processes in complex geological media. The codes were linked with modules representing the coupled thermo-mechanical and hydrologic-mechanical behavior of rocks. The coupling modules contain nonlinear stress versus permeability and porosity functions. These coupling modules could be exchanged with modules containing any other type of empirical or theoretical hydrologic-mechanical coupling relationship. We have demonstrated the usefulness of linked, sequentially coupled THM analyses for complex problems related to injection and storage of CO_2 in depleted reservoir.

2. THM coupled modeling approach

In a reservoir, the mechanical deformations and fluid flow are coupled to each other. This coupling can be significant in reservoirs containing compressible rock. Coupled reservoir geomechanics analyses aim to identify the mechanical deformations due to oil and gas extraction, and to simultaneously include the changes in fluid flow resulting from mechanical deformations in the reservoir rock. Fluid flow modeling involves sophisticated analyses that need to include multiple fluids and fluid components differentiated according to the molecular weight of the constituent hydrocarbon fluids. The fluids can undergo dissolution and chemical changes depending on the prevailing pressures and temperatures. The pressure of the fluid leads to modifications in the stress regime in the rock which in turn can give rise to rock deformations and strains.

The theoretical background of fluid flow and mechanical coupled processes is presented here, followed by an overview of coupling methods (Longuemare *et al.* 2002). Let us consider two equations discretized in time (dt): one describing the deformation of the rock mass, and the other one describing fluid flow in porous rock (see equations below, with coupling terms in red). When no coupling phenomenon is taken into account, forces (F) are related to displacements (u) with a compliance tensor [K] (geomechanics), and fluid flow (Q) is related to pressure changes (p) with a flow tensor [E] (reservoir modeling). Coupling is achieved when forces are also related to pressure changes and fluid flow is also related to displacements of the rock mass, both with a coupling tensor [L].

$$[K]d_t u + [L]d_t p = F \quad (1)$$

$$[L]^t d_t u + [E]d_t p = Q \quad (2)$$

In conventional flow simulators, only the fluid flow equation is solved. Pore volume variation is assumed to be only pressure dependent through a pore volume compressibility coefficient. Stress changes are therefore implicitly assumed, without being explicitly computed. In such simulators, reservoir permeability remains unaffected by pore pressure changes. Coupled equations can be solved via either partial or full coupling methods. Partial coupling methods make use of conventional flow and mechanical simulators through staggered coupling schemes. Each simulator solves one of the two equations, and data is exchanged at selected time steps. These methods take advantage of developments in conventional simulators, and they enable selection of different time steps for each simulator, hence reducing computational time. Full coupling methods solve simultaneously both equations. Efforts on developing such simulators are still ongoing. If a large number of iterations are performed with partial coupling methods, results can approach those obtained by full coupling methods.

In this study, a so-called two-way partial coupling method has been conducted in which the exchange at given time steps between the ECLIPSE finite difference reservoir simulator and the ABAQUS finite element mechanical simulator which explained in details below:

After acquiring the relevant data, the reservoir “static” model is built in the reservoir simulation software, ECLIPSE, which describes all its geological, lithological, stratigraphical and petrophysical aspects. After that the “dynamic” model is built in ECLIPSE which takes as input all the information of the static model and, by introducing a series of additional parameters regarding the characteristics of the fluids, the rock and the well system, provides the information required for the field management, such as the dynamic reserve evaluation injection and the production profiles as a function of the development scenarios (Fig. 1).

In order to simulate geomechanical process of a reservoir, mechanical parameters must be defined. The geomechanical modeling begins with the construction and calibration of a one-dimensional Mechanical Earth Model (1-D MEM) for each well using all the available data from logs, cores, images, drilling, etc.

A MEM is a numerical representation of the geomechanical knowledge available for a well which contains data and information about the various formations needed to make rock mechanical predictions (Plumb *et al.* 2000). The 1-D MEMs will provide the following as a continuous profile along the injection well trajectory at log-scale resolution:

•Mechanical stratigraphy (grain supported and clay supported deformation mechanisms);
•Rock properties (Young’s modulus, Poisson’s ratio, etc.);
•Rock strength parameters (UCS, Tensile strength, Friction Angle, Cohesion, etc.);
•The state of in-situ stresses (directions and magnitudes); and

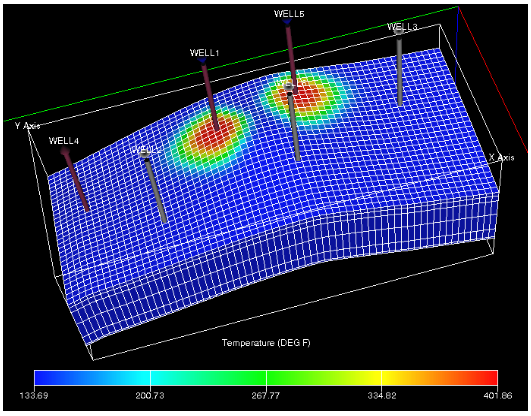

Fig. 1 3D dynamic model: reservoir temperature and wells system

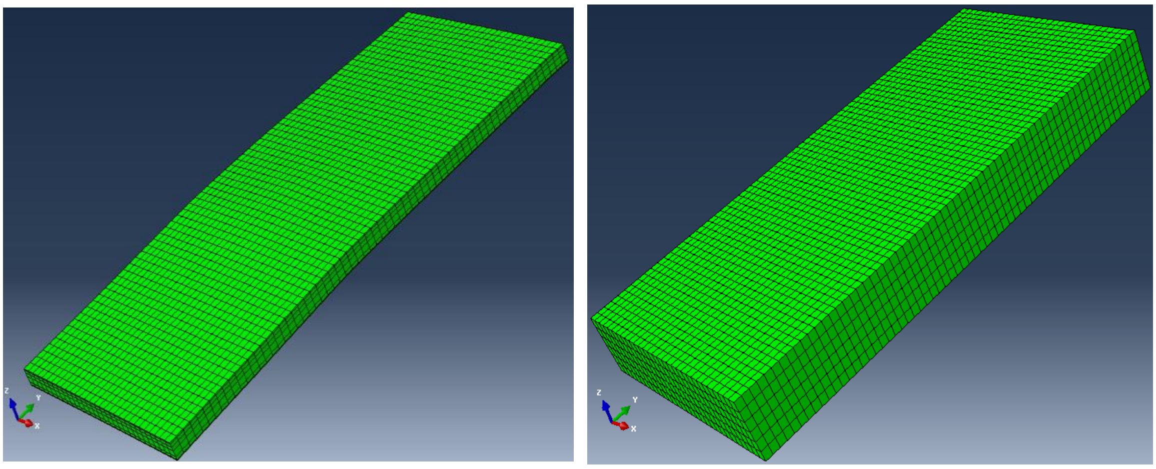

Fig. 2 3D geomechanical model: reservoir (left), and reservoir and its surrounding (right)

•Predicted pore pressure profile.

The data contained in the 1-D MEMs for each well will be calibrated and validated using the existing calibration data such as calipers, image logs, drilling, mini-frac, pore pressure, and laboratory core analysis data to constrain and reduce uncertainties in the 1-D model. Using these calibrated 1-D MEMs and other data such as seismic, a three-dimensional Mechanical Earth Model (3-D MEM) is developed for the entire field under consideration.

3-D MEM is constructed in the mechanical simulation software, ABAQUS, using the property model developed in the previous steps. The geomechanical calculation requires modeling not only of the reservoir but also of its containment (over-, under- and side-burden), to apply boundary conditions and to define the thermo-hydromechanical properties of the reservoir and surrounding rocks (Fig. 2).

So this 3-D model consists of reservoir, overburden, under-burden and side-burden up to sufficient distance to eliminate any boundary effects that may have on the results. Initial stress analysis is performed to model the far-field state of in-situ stress (pre-injection and pre-production state). The external part (side-burden, over-burden and under-burden) of the grid, needed to

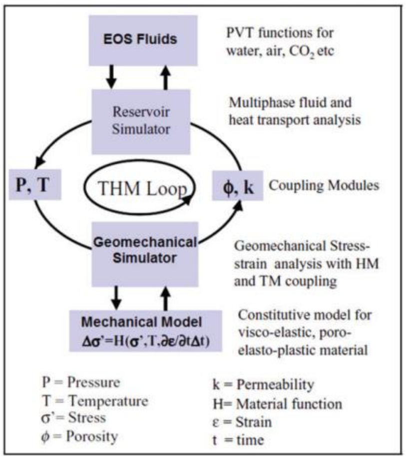

Fig. 3 THM loop (linking between ECLIPSE and ABAQUS)

correctly simulate the geomechanical behavior of the system, is automatically built by a MATLAB interface code provided that the final model size is given.

It is evident that solving the equations in this great environment, knowing that the majority of the models fall outside the reservoir, will impose enormous computational costs. As a result, it can be separated to two sets of equations that are used for inside and outside of the reservoir. Then, in the reservoir part the flow and equilibrium equations are solved completely assigning 8-node brick stress/displacement/pore pressure/temperature (C3D8PT) and in the outside of the reservoir only equilibrium equations are solved assigning 8-node brick stress/displacement (C3D8).

The initial geostatic stress field must be in equilibrium with the applied loads and boundary conditions. Ideally, the loads and initial stresses should exactly equilibrate and produce zero deformations. This state is obtained performing an initial ABAQUS analysis fixing all displacement degree of freedoms. The calculated reaction forces from the ABAQUS output file are then used to create nodal point forces, which are applied in the first step of the actual ABAQUS analysis.

An ECLIPSE to ABAQUS link takes multiphase pressures and temperature from ECLIPSE simulation and provides updated temperature, and pore pressure to FLAC3D (Fig. 3). Because an ECLIPSE mesh uses one grid-point within each element and in the built geomechanical model ABAQUS nodes are located in element corners, data have to be interpolated from mid-element (ECLIPSE) to corner locations (ABAQUS).

After data transfer, ABAQUS internally calculates thermal strain and effective stress according to

$$\Delta\varepsilon^T = I\beta_T\Delta T \tag{3}$$

$$\acute{\sigma} = \sigma + I\alpha P \tag{4}$$

where ε^T is thermal strain, β^T is the linear thermal expansion coefficient, I is the unit tensor, T in temperature, σ' is effective stress, σ is total stress, α is a Biot effective stress parameter (Biot 1941) and P is pore fluid pressure. In a multiphase flow calculation, the value of P transferred to

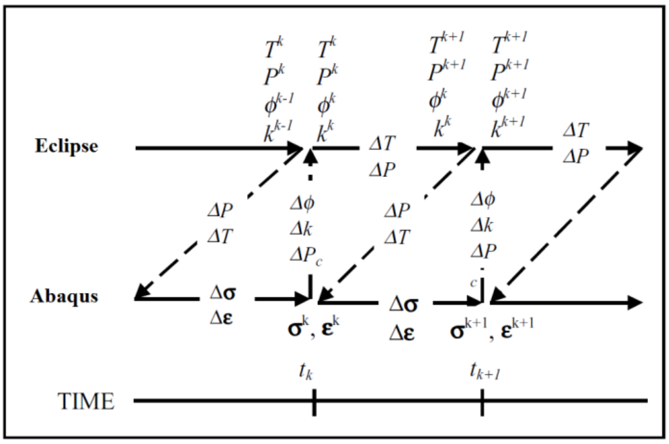

Fig. 4 Explicit sequential solutions of a linked ECLIPSE and ABAQUS simulation

ABAQUS could represent an average pore pressure calculated from the pressures of the various phases (Rutqvist *et al.* 2002). An ABAQUS to ECLIPSE link takes element stress or deformation from ABAQUS and corrects element porosity and permeability for ECLIPSE according to the following general expressions

$$\phi = \phi(\sigma', \varepsilon) \tag{5}$$

$$k = k(\sigma', \varepsilon) \tag{6}$$

The calculation is stepped forward in time with the transient TH analysis in ECLIPSE, and at each time step or at the ECLIPSE Newton iteration level, a quasi-static mechanical analysis is conducted with ABAQUS to calculate stress-induced changes in porosity and intrinsic permeability. The resulting THM analysis is explicit sequential, meaning that the porosity and permeability is evaluated only at the beginning of each time step. The ECLIPSE code is executed for a TH analysis between t^k to t^{k+1} until mass conservation is assured by solving ECLIPSE flow and heat equation (Fig. 4).

The reservoir pore pressure and temperature can be directly used in the geomechanics model (using mapping code). However, the volumetric strain in reservoir model cannot be directly used and different formulations of porosity and permeability are employed for this purpose. Experimental studies performed by Manguy and Longuemare (2002) and Touhidi-Baghini (1998) showed that changes in permeability and porosity are directly related to volumetric strains which are mainly caused by shear failure.

To account for changes in porosity and permeability due to volumetric strains developed in the rock by temperature and pressure, the following equations can be used

$$\phi = \phi_0 + \alpha(\varepsilon_v - \varepsilon_{v0}) + \frac{1}{\varphi}(P - P_0) \tag{7}$$

$$\ln\frac{k_1}{k_0} = \frac{c}{\phi_0}\varepsilon_v \tag{8}$$

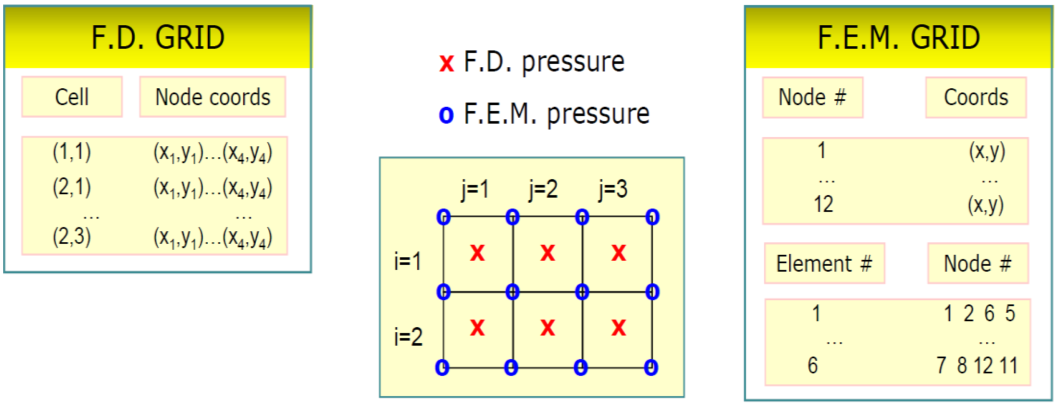

Fig. 5 Adjustment of finite difference and finite element mesh

where ϕ is porosity, ϕ_0 is initial porosity, k_1 is permeability, k_0 is initial permeability, P is pore pressure and ε_v is volumetric strain. Also, α and φ represent constant parameters (Biot 1941). The values for α and φ for the studied reservoir are one and infinite, respectively. Also, P_0 is the initial reservoir pore pressure and ε_{v0} represents the initial volumetric strain. An appropriate value for c has to be selected. Values for c are derived from the Chardabellas equation. According to Touhidi-Baghini, the values c = 5 and c = 2 appear to be appropriate to match with vertical and horizontal permeability evolutions, respectively (Touhidi-Baghini 1998). These coupling modules could be exchanged with modules containing any other type of empirical or theoretical thermo-hydro-mechanical coupling relationship.

In each steps the data must be mapped from reservoir grid to geomechanics grid and vice versa. The result of coupled solution will depend upon the mapping of information between the two grids.

The fact that the grid type in the reservoir simulator is different from geomechanical simulator makes the mapping process more complicated. In fact, in the reservoir simulator a finite difference grid discretization is used where flow variables are computed at the center of grid-blocks while in the geomechanical simulator a finite element grid discretization is used to compute displacements at the nodes of the grid (Fig. 5).

Generally, the reservoir grid in geomechanical simulator is not identical with the reservoir grid in the reservoir simulator. In the reservoir geomechanics simulator, the size of the grid cells is less than reservoir fluid flow simulator, i.e., the reservoir grid in reservoir simulator is coarser than the geomechanics grid which is necessary for accurate stress and strain determination.

Also in this research, the grids in the reservoir and geomechanical simulators are not coincident, passing the data (temperature, pressure, volumetric strain) between the two simulators is more complex. Therefore, a field transfer algorithm must be used to perform the passing of data from one grid to the other. Here, a development of MATLAB code is used for mapping the data from reservoir grid centers to geomechanics grid nodes and vice versa.

The lateral boundaries of the reservoir are considered with neither thermal nor fluid flow. The constraints for the geomechanical model are as follows. The right, left, front and back sides of the model are fixed in the x-direction and y-direction so there would be no displacement in the x and y directions. The bottom side of the model is fixed in all directions and the top of the model is free to move in all directions.

As a supercritical fluid, the CO_2 behaves like a gas with low viscosity but having a liquid-like density of 200–900 kg/m3, depending on pressure and temperature. Because the supercritical CO_2 is less dense than water, deep underground disposal requires that the caprock is sufficiently impermeable to trap the injected CO_2 for a sufficiently long time. Important rock-mechanical aspects of this simulation are to study the integrity of the caprock and the possibilities of rock failure.

3. Regional geological setting

A coupled flow, thermal, and geomechanical model has been developed in order to study the THM response of the injection on the reservoir and surrounding layer to increasing of pressure and reduction of temperature after CO_2 injection. The studied oil region situated in Khuzestan province was studied as the most oil-rich region in Iran, with the Dezful Embayment in southwest Khuzestan being especially prolific. Most of the oil fields in the region are located in the foothill zone (Zagros Folded zone) of the NW-SE trending Zagros Mountain range having similar trends to the Zagros Mountain range elongated anticline structure, which is called the Zagrous Trends.

The result of drilling in this field and neighborhood fields show that thirteen formations from three groups overlaying one another. The youngest group Fars Group consists of Aghajari and Gachsaran formations, Asmari, Pabdeh, and Gourpi formations, the middle group (Bangestan Group) consists of Ilam, Lafan, Sarvak, and Kazhdumi formations and the oldest group (Khami Group) consists of Darian, Gadvan and Fahliyan formations (Fig. 6).

The Sarvak limestone containing heavy oil is the main productive formation. The thickness and the layer slope of Sarvak formation are approximately constant. The reservoir is approximately 2500 m deep and 140 meters thick. Limestone is the dominant rock type in this reservoir. The reservoir geometry has been indicated by 3-D seismic measurements and six wells drilled in the structure. The mechanical properties and the initial stress profile are required to be incorporated in the geomechanical model and coupled with the flow model in order to be able to study the mutual effect of pressure, temperature and stresses and the resulting effect on integrity and injectivity. The reservoir rock mechanical parameters including, uniaxial compressive strength, Young’s modulus and Poisson’s ratio were obtained from Dipole sonic imager (DSI) logs, laboratory tests and empirical relationships.

The reservoir Young’s modulus, Poisson’s ratio, cohesion, friction angle is 20 GPa, 0.22, 3 MPa and 30 degrees, respectively. Also, the reservoir initial pressure is about 22 MPa and densities of water, oil and gas are 1190, 850 and 0.90 Kg/m^3, respectively. Other characteristics of the reservoir layers are given in Table 1.

Table 1 Mechanical property of the caprock and reservoir layers

Layer	Thickness (m)	Porosity(%)	Permeability(md)
1	10	1	<1
2	25	10	45
3	30	15	45
4	45	15	55
5	25	10	40
6	5	1	2

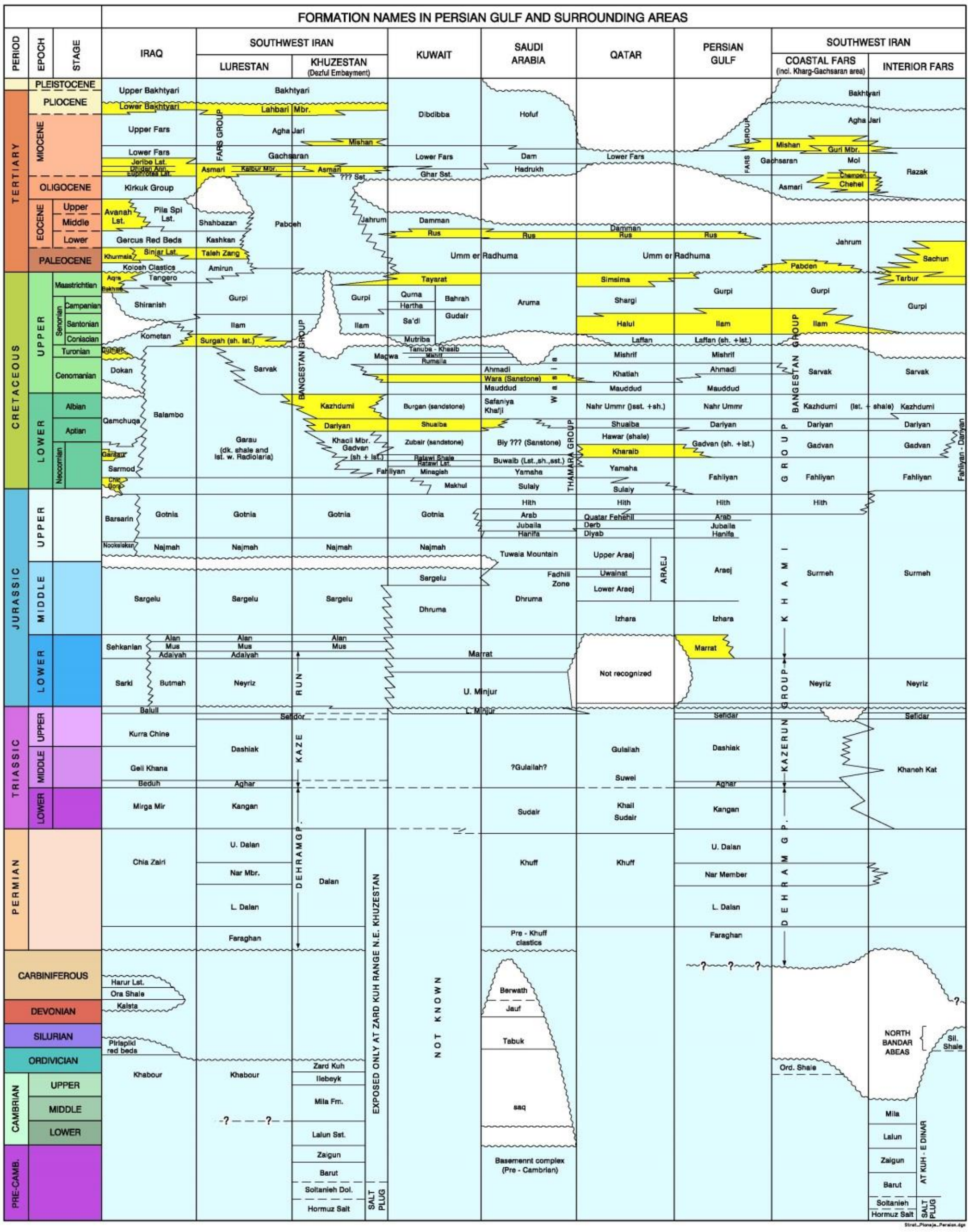

Fig. 6 Generalized Stratigraphic Column of SW IRAN and adjacent area (Setudehnia 1978)

4. Results from depletion and subsequent CO_2 injection simulation

The production of hydrocarbons from a reservoir implies that at the time of production there was sufficient porosity and permeability for large-scale fluid flow into a producing well; therefore it may be safe to assume a certain level of injectivity for the flow of CO_2 out of an injecting well into the reservoir. However, production may significantly alter the properties of the reservoir as well as the integrity of the seal. For these reasons, an important step in the evaluation of any reservoir for gas storage is to characterize the effects of production on the reservoir properties and seal integrity. After investigating the production effects on a field, we can make observations and predictions about the influence that injection will have on the reservoir and seal.

The studied reservoir was encountered by six wells. Firstly, oil is produced from all the wells until meeting economical limitation (listed below) and then the partially depleted reservoir will be used for CO_2 storage. The initial reservoir temperature is 135 degree Fahrenheit (F^o) and the reservoir was targeted using six wells. Production conditions and restrictions are as follow:

- Each well production minimum bottom hole pressure is 1300 Psi
- Oil production rate of each well is 2,500 stb/day (stock tank barrel per day)
- Oil production of each well terminated if the well production rate is less than 300 stb/day or water cut is more than 0.7.

Oil production of all wells started at January first 2007. When production from all the wells terminated (due to the above- mentioned restrictions) the wells No. 2, 3 and 6 will be used as injection wells. Injection strategy involves the injection of 100 MMscf/day (million standard cubic feet per day) by each well with an injection temperature of 80 F^o and a maximum bottom hole pressure of 4000 Psi.

The reservoir oil production rate is shown in Fig. 7. As shown in the Figure, at the beginning, each well production rate is 2,500 stb/day. As time passes, the oil production rate decreases gradually due to reservoir pressure reduction. After about 4000 days from the start of production, the production rates of wells No.1 and No.5 fall under the predefined limit, so their production will be terminated. Other wells will also be closed, so that after 10,500 days from the start of production, production from the reservoir will be stopped completely. Then the reservoir wells will be used as CO_2 injection wells.

Injection of CO_2 for geological storage will lead to increases in reservoir pressure. Since the studied reservoir has no fault, only caprock integrity is evaluated. Loss of caprock integrity could result in generating potential migration paths for the CO_2 into bounding formations. Therefore it is necessary to assess caprock integrity in the stage of the feasibility study.

Fig. 8 presents the calculated reservoir pressure during both production and injection period with consideration of the stress-dependent rock mass permeability and porosity (coupled THM

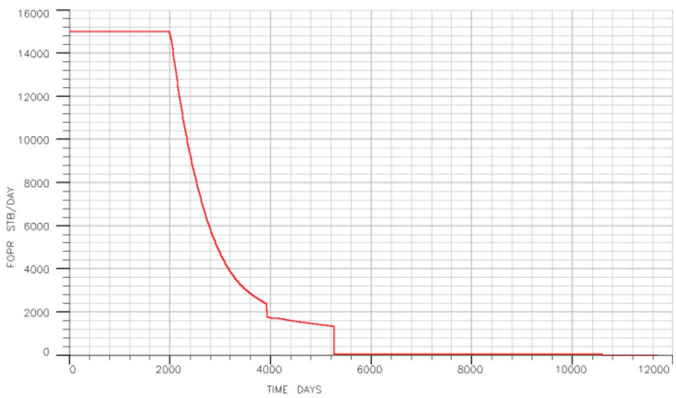

Fig. 7 Reservoir oil production rate

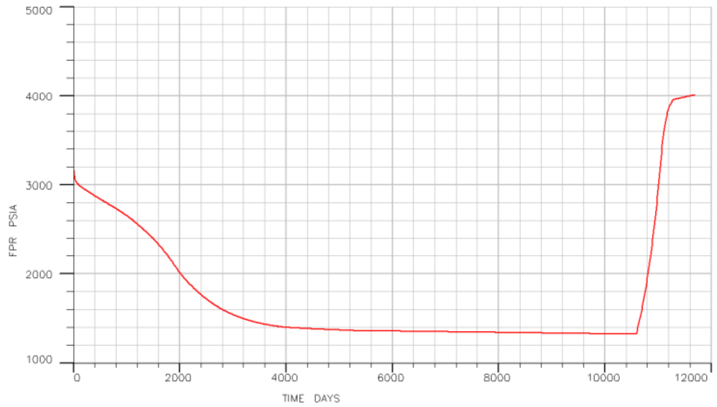

Fig. 8 Reservoir pressure rate

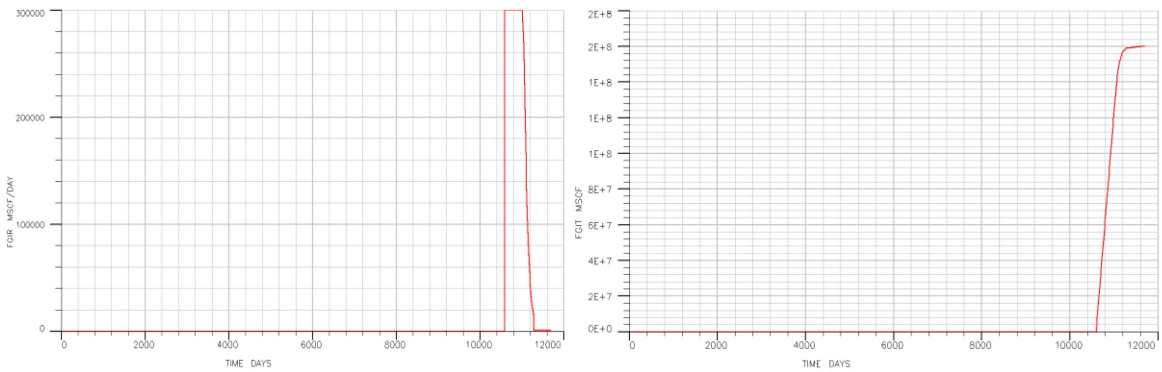

Fig. 9 Reservoir CO2 injection rate (left), and cumulative injection volume (right)

Table 2 Rock thermal properties (Eppelbaum *et al.* 2014)

Heat Capacity ($J.cm^{-3}.°C^{-1}$)	Thermal Conductivity ($W. m^{-1}.°C^{-1}$)	Thermal Expansion Coefficient ($°C^{-1}$)
2.30	2.37	2×10^{-5}

analysis). Also the reservoir CO_2 injection rate and cumulative injection volume are shown in Fig. 9.

Injection of CO_2 will cause formation pore pressure to increase, initially in the vicinity of the injector, then vertically and horizontally away from the injection well. The effective stress changes within the reservoir are predominantly controlled by the pore pressure changes and temperature change to a certain extent.

The in-situ stress regime for the case study is NF stress regime with stress ratio (k) of 0.75 and Mohr-Coulomb elasto-plastic failure criterion was used for geomechanical simulation of the reservoir and surrounding rock. The reservoir rock thermal properties are listed in Table 2.

The initial distribution of vertical stress and maximum principal stress are shown is Fig. 10.

As said before, CO_2 temperature is lower than the reservoir temperature. Therefore, the reservoir temperature decreases around the injection wells during injection. When temperature decreases, materials will contract (Fig. 11).

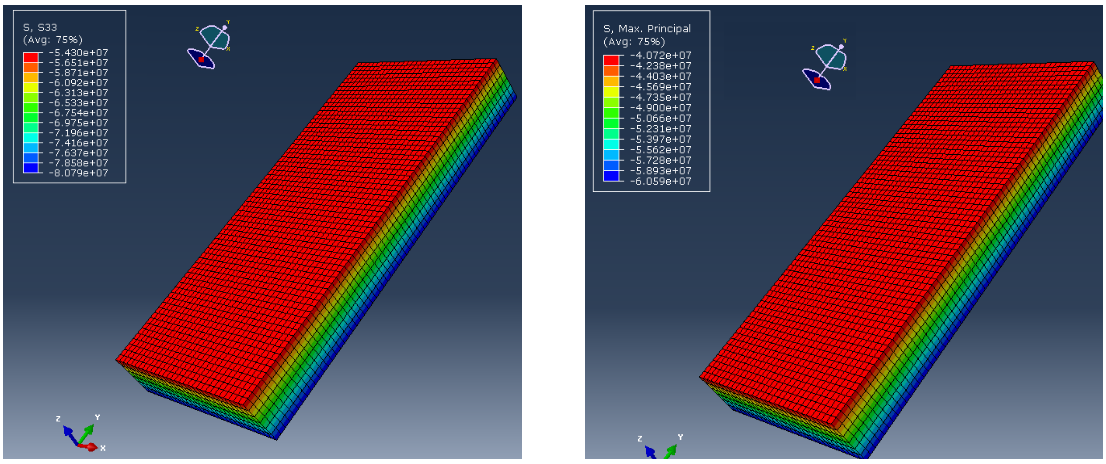

Fig. 10 Vertical stress (left), and maximum principal stress (right) distribution

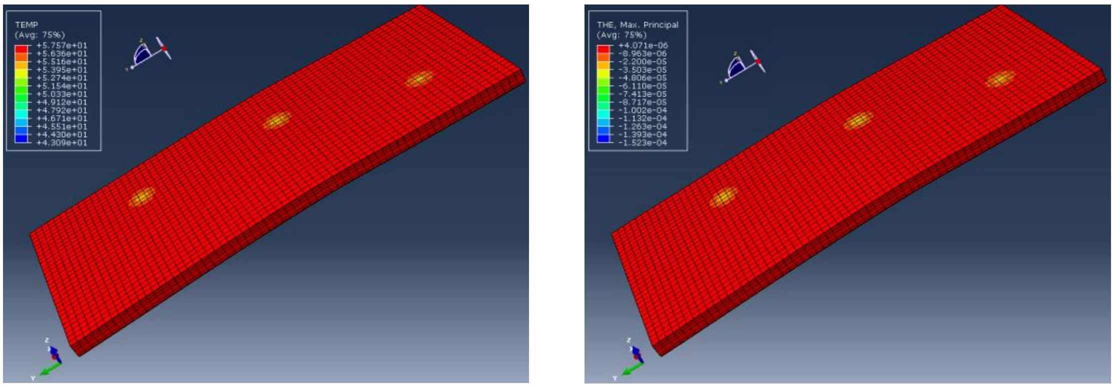

Fig. 11 Reservoir temperature distribution (left) and related maximum thermal strain (right)

For reservoir rocks, this gives rise to a decrease in the field stresses. The bottom-hole and near wellbore temperature is lower than the far-field-reservoir temperature during injection of fluids. The temperature drop will affect stresses around the wellbore and increases hydraulic fracturing potential in the near-wellbore region. The risk of thermal fracturing is even higher in the early injection (lower pore pressure) because of the reduction in the fracture gradient. In addition, reduction of the minimum effective stress due to thermal effects is larger for the lower reservoir layers. Therefore in case of dynamic fracture propagation, fracture growth would be larger for the lower reservoir layers due to larger cooling for these layers.

In addition to thermal effects corresponded to CO_2 injection, injection increases the pore pressure, dilates the rock skeleton and the pore fluid pressure modifies the in situ stresses in a complex set of interactions. In the caprock layer, effective minimum horizontal stress decreases in the vicinity of the injection well. In case of low strength materials and high injection pressure the possibility of failure of the caprock will occur first in the immediate vicinity of the injection wells. The stress change in the caprock is mainly caused by the stress change in the reservoir formations beneath it. Distribution of Von Mises stress during the coupling is shown on Fig. 12.

The finite element analysis of the reservoir and surrounding rock showed no sign of plastic

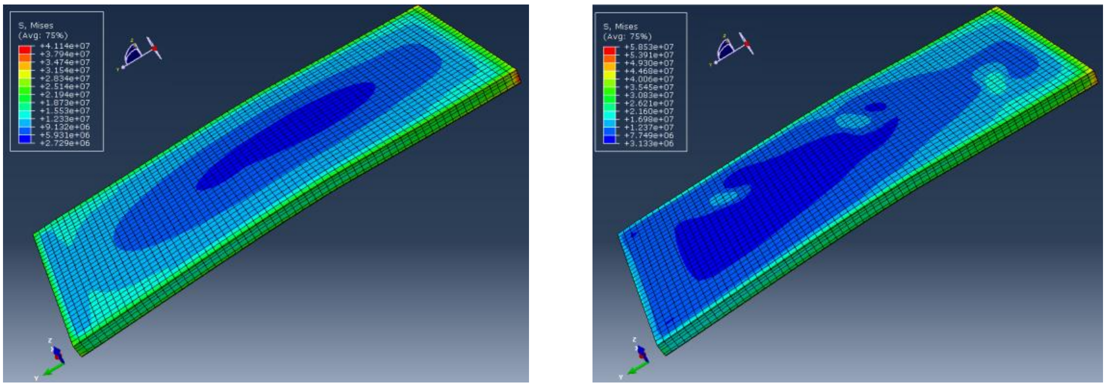

Partially depleted reservoir (after production) After CO_2 storage

Fig. 12 Mises stress distribution

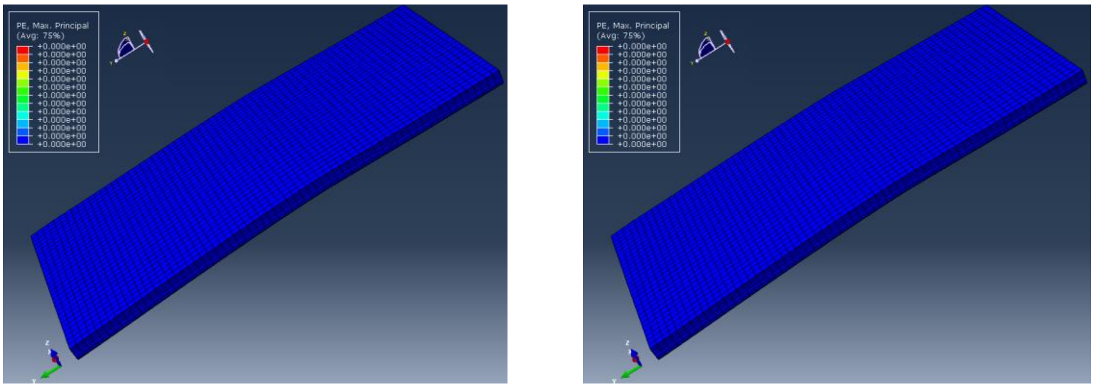

Partially depleted reservoir (after production) After CO_2 storage

Fig. 13 Maximum plastic strain

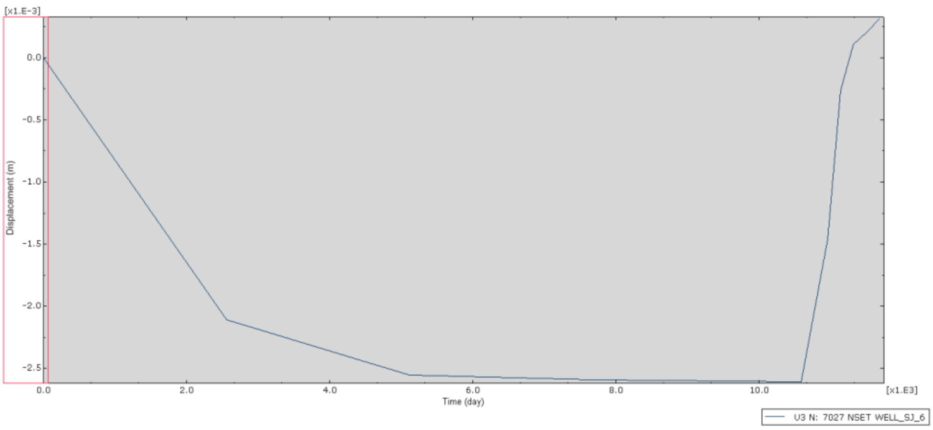

Fig. 14 Vertical displacement around WELL6

strain neither after production nor after CO_2 storage in any part of the caprock and reservoir itself (Fig. 13). During depletion and before the injection scenario, the caprock has shown subsidence.

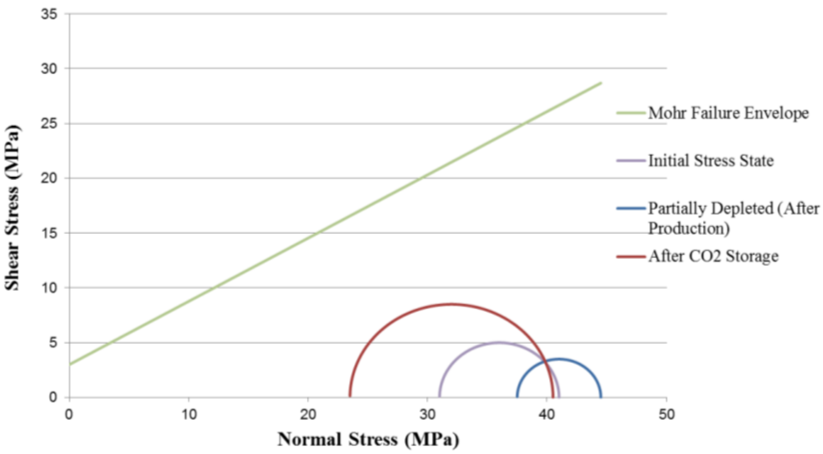

Fig. 15 WELL6 stress path

However by injection of, at the same time, the caprock displacement reversed (Fig. 14). Though, such displacements are ignorable because of less potential for instability of the caprock.

Variations in the caprock effective vertical stress and the shear stress were found to be small even in the vicinity of the injection wells as shown in Fig. 15 for WELL6 which is close to the anticline part of the caprock. Effective horizontal stress changes are too small to be seen in the stress variation maps.

Although the base case injection scenario would increase both the normal and shear stresses in the caprock, the increase is not significant enough to cause any failure in the caprock. The modeled injection scenario will neither cause tensile failure nor shear failure in the caprock and reservoir itself. This means that the injection scenario is safe to the integrity of the caprock from geomechanics point of view. However, other processes, such as chemical processes which are not considered in this study may also alter the mechanical and hydraulic properties of rock. It is recommended that the effects of these processes be also considered for a thorough analysis of caprock integrity.

5. Conclusions

In this paper, the two software ECLIPSE and ABAQUS were linked with modules representing the coupled thermo-mechanical and hydrologic-mechanical behavior of rocks. The main goal of this study will be the development of a complete and widely applicable workflow for integrating geomechanics, the evolution of reservoir and seal conditions and CO_2 sequestration.

The fluid flow simulator was initially executed over a first period (built static and dynamic model). Updated pore pressures at the end of this first period are interpolated and transferred onto the geomechanics grid in the geomechanical simulator using MATLAB code. Based on the updated producing conditions and constitutive relationships, the geomechanical simulator calculates the strains. Then, the reservoir permeability and porosity are modified according to theoretical or empirical functions (between volumetric strain, permeability and porosity). Updated grid block permeabilities and porosities are then transferred to the fluid flow simulator for the execution of the next time period. It was demonstrated that the usefulness of linked, explicit coupled THM analyses for complex problems was associated with CO_2 sequestration in a reservoir. The following conclusions can be drawn for the given parameters and production and injection scenarios through the analysis of the time history study of petrophysical parameters, effective stress and strain:

- The injection scenario will neither cause tensile failure nor shear failure in the caprock. In other words, the injection scenario is safe to the integrity of the caprock from geomechanics point of view.
- During the initial stages of CO_2 injection, there is potential for a significant reduction in the temperature in the near injection wells region, from 135 F^o to 80 F^o, which will further increase shear stress comparing normal stress in the cap rock. Since the formation has no fault, no instability occurs. But in case of faulted reservoirs, it is advisable to place injection wells in fault-free zones in order to reduce the risk of fault reactivation.
- When injecting a fluid below isothermal fracture pressure with a temperature below reservoir temperature, the fracture pressure will decrease due to reduction in minimum horizontal stress
- Repressurization of partially depleted reservoir to a pressure level close to the initial pore pressure results in reverse of the stress changes induced by production and restores the initial state of stress. Through injection, displacement also reversed.

References

Biot, M.A. (1941), “General theory of three dimensional consolidation”, *J. Appl. Phys.*, **12**(2), 155-164.

Chadwick, R.A., Williams, G.A., Williams, J.D.O. and Noy, D.J. (2012), “Measuring pressure performance of a large saline aquifer during industrial scale CO_2 injection: the Utsira Sand, Norwegian North Sea”, *Int. J. Greenhouse Gas Control*, **10**, 374-388.

Elyasi, A., Goshtasbi, K. and Hashemolhosseini, H. (2016), “A coupled thermo-hydro-mechanical simulation of reservoir CO_2 enhanced oil recovery”, *Energy Environ.*, **27**(5), 524-541.

Elyasi, A., Goshtasbi, K., Hashemolhosseini, H. and Barati, S. (2016), “Coupled solid and fluid mechanics simulation for estimating optimum injection pressure during reservoir CO_2-EOR”, *Struct. Eng. Mech.*, **59**(1), 37-57.

Elyasi, A., Goshtasbi, K. and Hashemolhosseini, H. (2016), “A coupled geomechanical reservoir simulation analysis of CO_2– EOR: A case study”, *Geomech. Eng.*, **10**(4), 423-436.

Eppelbaum, L., Kutasov, I. and Pilchin, A. (2014), *Thermal Properties of Rocks and Density of Fluids*, in *Applied Geothermics*, Springer, Berlin, Heidelberg, Germany.

Goodarzi, S., Settari, A., Zoback, M. and Keith, D. (2010), “Thermal aspects of geomechanics and induced fracturing in CO_2 injection with application to CO_2 sequestration in Ohio river valley”, *Proceedings of the Society of Petroleum Engineers International Conference on CO_2 Capture, Storage, and Utilization*, Louisiana, U.S.A., November.

Hoffert, M.I., Caldeira, K., Benford, G., Criswell, D.R., Green, C., Herzog, H., Jain, A.K., Kheshgi, H.S., Lackner, K.S., Lewis, J.S., Lightfoot, H.D., Manheimer, W., Mankins, J.C., Manuel, M.E., Perkins, L.J., Schlesinger, M.E., Volk, T. and Wigley, T.M.L. (2002), “Advanced technology paths to global climate stability: Energy for a greenhouse planet”, *Science*, **298**(5595), 981-987.

House, K.Z., Schrag, D.P., Harvey, C.F. and Lackner, K.S. (2006), “Permanent carbon dioxide storage in deep-sea sediments”, *Proc. Nat. Acad. Sci.*, **103**(33), 12291-12295.

IPCC (2007), *Summary for Policymakers*, in *Climate Change 2007: The Physical Science Basis*, Contribution of Working Group I to the Fourth Assessment Report of the Intergovernmental Panel on Climate Change, Cambridge University Press, Cambridge, U.K. and New York, U.S.A.

Longuemare, P., Mainguy, M., Lemonnier, P., Onaisi, A., Gérard, C. and Koutsabeloulis, N. (2002),

"Geomechanics in reservoir simulation: Overview of coupling methods and field case study", *Oil Gas Sci. Technol.*, **57**(5), 471-483.
Mainguy, M. and Longuemare, P. (2002), "Coupling fluid flow and rock mechanics: formulations of the partial coupling between reservoir and geomechanical simulators", *Oil Gas Sci. Technol.*, **57**(4), 355-367.
Pacala, S. and Socolow, R. (2004), "Stabilization wedges: Solving the climate problem for the next 50 years with current technologies", *Science*, **305**(5686), 968-971.
Plumb, R.A., Edwards, S., Pidcock, G. and Lee, D. (2000), "The mechanical earth model concept and its application to high-risk well construction projects", *Proceedings of the IADC/SPE Drilling Conference*, New Orleans, Louisiana, U.S.A., February.
Rutqvist, J., Wu, Y.S., Tsang, C.F. and Bodvarsson, G. (2002), "A modeling approach for analysis of coupled multiphase fluid flow, heat transfer, and deformation in fractured porous rock", *Int. J. Rock Mech. Min. Sci.*, **39**(4), 429-442.
Setudehnia, A. (1978), "The Mesozoic sequence in southwest Iran and adjacent area", *J. Petrol. Geol.*, **1**(1), 3-42.
Touhidi-Baghini, A. (1998), "Absolute permeability of McMurray formation oil sands at low confining stresses", Ph.D. Dissertation, University of Alberta, Alberta, Canada.

CC